



# The moderate oxidative stress induced by glyphosate is not detected in *Amaranthus palmeri* plants overexpressing EPSPS

Mikel Vicente Eceiza, Miriam Gil-Monreal, María Barco-Antoñanzas, Ana Zabalza, Mercedes Royuela\*

Institute for Multidisciplinary Research in Applied Biology (IMAB), Public University of Navarre, Campus Arrosadia s/n, 31006, Pamplona, Spain

## ARTICLE INFO

### Keywords:

Oxidative Stress  
Glyphosate  
Herbicide mode of action

## ABSTRACT

The present study aimed to determine whether glyphosate-induced oxidative stress is directly related to the action mechanism of this herbicide (5-enolpyruvylshikimate-3-phosphate synthase or EPSPS inhibition) and analyse the role of oxidative stress in glyphosate toxicity of the weed *Amaranthus palmeri* S. Wats. Two kinds of populations were studied using EPSPS amplification: glyphosate-sensitive and glyphosate-resistant (by gene amplification). Plants were grown hydroponically and treated with different glyphosate doses, after which several oxidative stress markers were measured in the leaves. Untreated, sensitive and resistant plants showed similar values for the analysed parameters. Treated glyphosate-sensitive plants showed an increase in shikimate, superoxide and H<sub>2</sub>O<sub>2</sub> contents and dose-dependent lipid peroxidation and antioxidant responses; however, none of these effects were observed in resistant plants, indicating that glyphosate-induced oxidative stress is related to EPSPS inhibition. Oxidative stress is associated with an increase in the activity of peroxidases due to EPSPS inhibition, although the link between both processes remains elusive. The fact that some glyphosate doses were lethal but did not induce major oxidative damage provides evidence that glyphosate toxicity is independent of oxidative stress.

## 1. Introduction

Weed control is a challenging issue in modern agriculture. Although many methods have been implemented to minimise or avoid the problems associated with weeds, herbicides continue to be the most extensively used tools for weed control (Edwards and Hannah, 2014). Among all herbicides, glyphosate is the most widely used worldwide since it can now be used as a selective herbicide, since the commercialisation of glyphosate-resistant crops in the mid-1990s (Duke, 2018). Its mechanism of action involves inhibition of 5-enolpyruvylshikimate-3-phosphate synthase (EPSPS), a key enzyme in the biosynthetic aromatic amino acid (AAA) pathway. EPSPS converts shikimate-3-phosphate (S3P) and phosphoenolpyruvate (PEP) to 5-enolpyruvylshikimate-3-phosphate (EPSP) in plastids, a necessary stage for the biosynthesis of the AAAs tyrosine (Tyr), phenylalanine (Phe), and tryptophan (Trp).

Nevertheless, glyphosate toxicity is not restricted to its interaction with the target site. The metabolic roadblock caused by EPSPS inhibition carries physiological consequences that eventually lead to plant death (Gomes et al., 2014). The physiological effects of glyphosate include the

accumulation of shikimate, quinate, and total free amino acids (Fernández-Escalada et al., 2016; Orcaay et al., 2010). This can be considered direct results of the deregulation of the shikimate pathway, as well as common generic stress markers such as loss of photosynthetic efficiency (da Silva Santos et al., 2020) or ethylene accumulation (Einhart et al., 2020; Lee and Dumas, 1983). The physiological downfall generated by glyphosate treatment alters the internal content of many phytohormones (including indol-3-acetic acid and abscisic acid) and global gene expression profiling related to biosynthesis and transport of phytohormones (Doğramaci et al., 2017; Jiang et al., 2013).

Oxidative stress caused by the overproduction of reactive oxygen species (ROS) is also a common response to different abiotic and biotic stresses, and it manifests as oxidative damage in biomolecules or changes in antioxidant activity. Under adequate conditions, ROS production is balanced by antioxidant activity; however, under stress conditions, ROS are overproduced and accumulated, which leads to the aforementioned oxidative damage and/or induction of the antioxidant systems (Demidchik, 2015). Several herbicides, such as glufosinate (Caverzan et al., 2019; Takano et al., 2019), have been reported to cause

\* Corresponding author.

E-mail address: [royuela@unavarra.es](mailto:royuela@unavarra.es) (M. Royuela).

<https://doi.org/10.1016/j.jplph.2022.153720>

Received 4 February 2022; Received in revised form 10 May 2022; Accepted 10 May 2022

Available online 13 May 2022

0176-1617/© 2022 The Authors. Published by Elsevier GmbH. This is an open access article under the CC BY license (<http://creativecommons.org/licenses/by/4.0/>).

oxidative stress in plants. In the case of glyphosate, numerous studies have shown that oxidative stress is a secondary effect of herbicide exposure, manifested in ROS production and accumulation, lipid peroxidation, protein oxidation, increase of non-enzymatic and enzymatic antioxidant activity, changes in redox-related gene expressions and disruption of ascorbate-glutathione pathway (Ahsan et al., 2008; de Freitas-Silva et al., 2017; Gomes and Juneau, 2016). Nevertheless, both its origin (whether it is directly or indirectly linked to EPSPS inhibition or a separate side effect) and the role of oxidative damage in the physiological downfall that leads to the death of treated plants are yet unknown.

Despite the ignorance of the exact mechanism of plant death after glyphosate treatment (from EPSPS inhibition to plant death), the efficacy of this herbicide and the introduction of genetically modified crops resistant to glyphosate are the reasons behind its massive usage. Consequently, some weed populations have developed glyphosate resistance. To date, at least one glyphosate-resistant population belonging to 53 species has been identified (Heap, 2022). One of these species is *Amaranthus palmeri* S. Wats., a C4 weed which is extremely difficult to control owing to its fast growth, rapid seed dispersal, and great genetic variability that enables it to develop resistance to herbicides (Vélez-Gavilán, 2019). In the majority of glyphosate-resistant populations of *A. palmeri*, EPSPS gene amplification is the mechanism of resistance (Gaines et al., 2019). Gene amplification of EPSPS leads to massive production of the enzyme; thus, the recommended glyphosate field dose is not enough to inhibit EPSPS activity and thus does not kill the plant (Fernández-Escalada et al., 2016; Gaines et al., 2010). Although the resistance mechanism is well established, knowledge regarding the physiological background or possible physiological effects of glyphosate exposure on these resistant weeds is limited. The availability of a biotype overexpressing the EPSPS enzyme provides an opportunity to analyse how EPSPS overexpression affects the response of oxidative status to glyphosate in comparison with a sensitive population.

This study aimed to determine whether oxidative stress caused by glyphosate is detected in resistant *A. palmeri* plants overexpressing EPSPS, while evaluating the role of oxidative stress in glyphosate toxicity. To this end, shikimate content, several oxidative damage markers, ROS content, and antioxidant activity were compared between two *A. palmeri* populations (glyphosate-sensitive and glyphosate-resistant with EPSPS amplification) treated with different glyphosate doses.

## 2. Materials and methods

### 2.1. Plant material and treatment application

The seeds of both glyphosate-sensitive (S) and resistant (R) *A. palmeri* biotypes were originally collected from North Carolina (USA) and provided by Dr. Gaines (Colorado State University, Fort Collins, CO, USA). The target site-resistance mechanism of the resistant population was EPSPS gene amplification, as R individuals had a mean 47.5-fold increase in the number of copies of the EPSPS gene which led to a 25-fold increase in the level of this protein and a 26-fold increase in EPSPS activity, compared to S individuals. No other phenotypic differences have been detected between both populations (Fernández-Escalada et al., 2016, 2017, 2019).

Plants were cultivated and grown hydroponically according to Fernández-Escalada et al. (2016). Seeds were surface-sterilised before germination (Labhili et al., 1995). For germination, the seeds were incubated for 4 days at 4 °C in the dark. They were then subjected to a 60 h light/dark cycle of 16 h/8 h at 30 °C/18 °C. After germination, plants were transferred to aerated 2.7 L hydroponic tanks in a phytotron (day/night, 16 h/8 h; light intensity, 0.5 mmol s<sup>-1</sup> m<sup>-2</sup> PAR; temperature, 22/18 °C; relative humidity, 60/70%). The plants remained at the vegetative phenological stage throughout the experiment. Nutrient solution (Hoagland and Arnon, 1950) was supplemented with 15 mM

KNO<sub>3</sub>.

Plants of each population were treated with a different range of glyphosate doses, due to the different sensitivity to the herbicide, which were determined in previous experiments. S plants were treated with 0.5 times the recommended field rate (0.5 FR), FR, 2 times the FR (2 FR), and 3 times the FR (3 FR); meanwhile, R plants were treated with FR, 2 FR, 3 FR, and 6 FR.

Glyphosate is recommended at 0.84 kg ha<sup>-1</sup> (Culpepper et al., 2006). Fortin Green® (Key, Tárrega, CAT, Spain) was used as the commercial herbicide. Plants were treated after reaching the growth stage defined as BBCH 14.35 (19–22 days old). 2.52 mL of the herbicide solution per tank (4.59 dm<sup>2</sup>) was sprayed using an aerograph (model Definik, Sagola, Vitoria-Gasteiz, EUS, Spain) connected to a compressor (model Werther, Breverrato, Italy; 60 W, 10 L m<sup>-1</sup>, 2.5 bar). Untreated plants of each population were sprayed with water using the same aerograph and compressor. The experiment was performed twice.

### 2.2. Analytical determinations

The leaves were sampled three days after herbicide treatment, frozen in liquid N<sub>2</sub>, and stored at –80 °C. Leaves from the same plant individual were collected together and considered as a biological replicate. The samples were powdered using a Retsch mixer mill (MM200, Retsch, Haan, Germany), and the amount of tissue required for each analytical determination was separated. For ROS detection, disks with 10 mm diameter were excised from fresh leaves five days after herbicide treatment. Several treated plants from each population were left in the phytotron to determine the lethality of the applied glyphosate doses.

#### 2.2.1. Shikimate content in leaf disks

Three leaf disks (4 mm diameter) were excised from the youngest leaf of each plant for shikimate content determination. Leaf disks were placed in 2 mL Eppendorf tubes and stored at –80 °C until analysis. Shikimate was extracted as described previously, and the shikimate content was quantified spectrophotometrically at 380 nm (Fernández-Escalada et al., 2016).

#### 2.2.2. Presence of ROS

O<sub>2</sub><sup>-</sup> was localised *in situ* by nitro blue tetrazolium (NBT) staining of the leaf disks (Romero-Puertas et al., 2004). Leaf disks of 10 mm diameter were immersed in a 0.1% (w/v) solution of NBT in a 50 mM potassium phosphate buffer (pH 6.4), containing 10 mM Na-azide. Then, the disks were vacuum-filtrated for 10 min and illuminated until the appearance of blue formazan precipitates, which appear as dark blue spots.

H<sub>2</sub>O<sub>2</sub> was localised *in situ* via 3,3'-diaminobenzidine (DAB) staining of leaf disks (Daudi and O'Brien, 2012). Leaf disks of 10 mm diameter were immersed in 0.1% (w/v) solution of DAB, containing 200 mM HCl, 0.05% (v/v) Tween 20, and 200 mM Na<sub>2</sub>HPO<sub>4</sub> (Daudi and O'Brien, 2012). The disks were then vacuum-filtrated for 10 min and incubated overnight in the dark. Disks were illuminated until a brown precipitate was formed by the reaction of DAB with H<sub>2</sub>O<sub>2</sub>.

Leaf disks from both assays were faded by immersion in boiling ethanol and stabilised in 10% (v/v) glycerol. Leaf disks were scanned using a GS-800 densitometer and O<sub>2</sub><sup>-</sup> and H<sub>2</sub>O<sub>2</sub> deposits were quantified using the Quantity One software (Bio-Rad, Hercules, CA, USA).

#### 2.2.3. Lipid peroxidation

Lipid peroxidation was determined by spectrophotometric detection of malondialdehyde (MDA) (Hodges et al., 1999). Samples (0.05 g) were homogenised in 1 mL 0.1% (w/v) TCA and mixed with a reagent solution comprising 20% (w/v) TCA, 0.01% (w/v) butylated hydroxytoluene, and 0.65% (w/v) thiobarbituric acid (TBA). The samples were then boiled at 95 °C for 25 min. The MDA-TBA complex content was measured at 532 nm, and corrections for unspecific turbidity and sugar-TBA complexes were performed by subtracting the absorbance of

the same sample at 600 and 400 nm, respectively (Hodges et al., 1999; Verma and Dubey, 2003).

#### 2.2.4. Protein carbonylation

Protein carbonylation was determined by the immunochemical detection of carbonyls (Romero-Puertas et al., 2002; Yan et al., 1998). Samples (0.1 g) were homogenised in a 0.3 mL protein extraction buffer comprising 100 mM potassium phosphate buffer (pH 7.4), 1 mM ethylenediaminetetraacetic acid (EDTA), and 0.2% (v/v) Triton x-100, containing freshly added 4.9 mM dithiothreitol, 2 mg mL<sup>-1</sup> polyvinylpyrrolidone (PVPP), and 1:100 diluted protease inhibitor cocktail from Sigma-Aldrich Co. (St Louis, MO, USA). The protein (0.5 mg) was incubated with 10 mM 2, 4-dinitrophenylhydrazine (DNPH) in 2 M HCl for 1 h at room temperature. Proteins were precipitated with 10% (w/v) TCA, and pellets were carefully washed with ethanol/ethyl acetate (1/1) two times. The pellets were resuspended in 10 mM sodium phosphate buffer (pH 7.4). Protein separation was performed using standard techniques (Corpas et al., 1998). Carbonylated proteins were detected using antibodies against DNPH (Sigma-Aldrich). Finally, carbonyl groups in proteins were visualised using the alkaline phosphatase method (Fernández-Escalada et al., 2017). The membranes and Coomassie gels were scanned using a GS-800 densitometer, and the intensity of the bands was quantified using the Quantity One software (Bio-Rad, Hercules, CA, USA). Protein carbonyl groups were quantified by membrane band intensity and normalised to the total protein content.

#### 2.2.5. Antioxidant capacity

Antioxidant capacity was measured using two different assays: 2,2-azino-bis (3-ethyl-benzothiazoline-6-sulfonic acid) (ABTS) and 2,2-diphenyl-1-picrylhydrazyl (DPPH). For the ABTS assay, the method of (Arnao et al., 2001) was followed, with slight modifications. Samples (0.05 g) were homogenised in a 0.5 mL 70% ethanol (v/v) solution containing 1% HCl (v/v) (Pérez-López et al., 2014). Samples were filtered with 450 nm filters and diluted to 1:10 in ethanol. These results were valid for both ABTS and DPPH assays. The stock solution for the ABTS assay consisted of 7.5 mM ABTS and 140 mM potassium persulfate ethylic solution diluted serially (as needed for achieving the absorbance value of 0.7 units at 734 nm). Antioxidant capacity was measured at 734 nm as the scavenging of ABTS radical cations and expressed as Trolox equivalent antioxidant capacity (TEAC). A linear standard curve was prepared with 0.03–0.5 mM Trolox. For the DPPH assay, the method proposed by Brand-Williams et al. (1995) was followed with some modifications. The stock solution comprised 0.2 mM DPPH ethylic solution incubated in darkness for 3.5 h. Antioxidant capacity was measured at 515 nm as the scavenging of DPPH and expressed as Trolox equivalent antioxidant capacity (TEAC). This mixture consisted of a stock solution, 40 mM Tris-HCl (pH 7.4), and a sample extract. A linear standard curve was made with 0.05–0.75 mM Trolox.

#### 2.2.6. Glutathione and related compounds

Glutathione was extracted from the samples (0.1 g) in 1 mL of 1 M HCl, derivatised with 5-iodoacetamide fluorescein, and reduced with tributylphosphine (Zinellu et al., 2005). Glutathione content was measured using a CE equipped with a laser-induced fluorescence detector (Zulet et al., 2015).

Reduced glutathione (GSH) levels were determined directly by the injection of an aliquot in the CE. Another aliquot was reduced with 10% tributylphosphine, and then total GSH, cysteine, and  $\gamma$ -glutamyl-cysteine were analysed by CE. Oxidised glutathione (GSSG) was determined as the difference between the total and reduced GSH values.

#### 2.2.7. Ascorbate

Ascorbate was extracted from samples (0.05 g) in 0.3 mL ice cold 2% meta-phosphoric acid containing 1 mM EDTA (Schützendübel et al., 2002). The homogenate was filtered through a 0.22  $\mu$ m Millex GV filter. Ascorbate was analysed by high-performance CE in a Beckman Coulter

P/ACE MDQ (Fullerton, CA, USA) associated with a diode array detector (Herrero-Martínez et al., 2000) and equipped with the P/ACE station software for instrument control and data handling.

Reduced ascorbate levels were directly determined by injecting an aliquot into the CE. Dehydroascorbate (DHA) was reduced with 200 mM dithiothreitol and total ascorbate content was analysed using CE. DHA was determined as the difference between the ascorbate values.

#### 2.2.8. Antioxidant enzymes

For antioxidant enzymatic activities, except ascorbate peroxidase (APX), samples (0.1 g) were homogenised in a 0.3 mL extraction buffer comprising 50 mM Tris-HCl (pH 7.4), 0.1 M EDTA, 0.2% (w/v) Triton x-100, and 10% (v/v) glycerol, containing freshly added 2 mM dithiothreitol, 1 mM phenylmethylsulfonyl fluoride (PMSF), and 1 mg mL<sup>-1</sup> PVPP. The assay mixture was desalted using Sephadex G-50. Peroxidase (POX) activity was measured using guaiacol as a substrate. The reaction mixture comprised a 50 mM potassium phosphate buffer (pH 6.1), 1% (v/v) guaiacol, 0.07% (v/v) H<sub>2</sub>O<sub>2</sub>, and a sample extract. The increase in absorbance due to the oxidation of guaiacol was measured at 470 nm. Catalase (CAT) activity was measured as the disappearance of H<sub>2</sub>O<sub>2</sub>. The reaction mixture consisted of 100 mM potassium phosphate buffer (pH 6.8), 40 mM H<sub>2</sub>O<sub>2</sub>, and the sample extract. The decrease in absorbance owing to the disappearance of H<sub>2</sub>O<sub>2</sub> was measured at 280 nm. Glutathione reductase (GR) activity was measured using NADPH as a substrate. The reaction mixture consisted of 48 mM HEPES buffer (pH 7.8), 1.4 mM MgCl<sub>2</sub>, 0.5 mM EDTA, 0.3 mM glutathione disulfide, 1.4 mM NADPH, and desalted sample extract. The decrease in absorbance due to NADPH oxidation was measured at 340 nm. Superoxide dismutase (SOD) activity was measured as the disappearance of superoxide formed by the reaction between xanthine and xanthine oxidase (XOD). The reaction mixture comprised a 45 mM potassium phosphate buffer (pH 7.8), 0.089 mM EDTA, 0.013 mM previously oxidised cytochrome c, 0.096 mM xanthine, and desalted sample extract. A variable amount of xanthine oxidase (depending on how much it was needed to reach a slope of 20 mOD min<sup>-1</sup>) was added before the measurement. The increase in absorbance owing to the disappearance of superoxide was measured at 550 nm. Finally, for APX activity, samples (0.05 g) were homogenised in a 0.15 mL extraction buffer comprising 100 mM potassium phosphate buffer (pH 7.5) and 1 mM ascorbic acid. APX activity was measured using the disappearance of H<sub>2</sub>O<sub>2</sub>. The reaction mixture comprised 41 mM phosphate buffer (pH 7), 0.4 mM ascorbic acid, 14.5 mM H<sub>2</sub>O<sub>2</sub>, and the sample extract. The decrease in absorbance owing to the disappearance of H<sub>2</sub>O<sub>2</sub> was measured at 280 nm. The results of all enzymatic activities were related to the total soluble protein measured in the same extracts (Bradford, 1976). A Synergy™ HT Multi-Detection Microplate Reader (BioTek Instruments Inc., Winooski, VT, USA) was used for absorbance measurements.

SOD isoenzymes were characterised by SOD activity staining (Beauchamp and Fridovich, 1971; Bridges and Salin, 1981). Electrophoresis was performed on 15% acrylamide gels, followed by the photochemical method of Beauchamp and Fridovich (1971) to localize SOD activity. The three isoenzymes (MnSOD, CuZnSOD, and FeSOD) were distinguished by their different sensitivities to the inhibitors KCN (inhibits CuZnSOD) and H<sub>2</sub>O<sub>2</sub> (inhibits CuZnSOD and FeSOD). Inhibitors were added to the staining solution before adding to the gels, and the gels were incubated in the staining solution for 70 min before exposure to light. The presence of the same amount of protein was confirmed by Coomassie Brilliant Blue staining of parallel gels. The gels were scanned with a GS-800 densitometer, and the intensity of the bands was quantified using the Quantity One software (Bio-Rad, Hercules, CA, USA). Different isoenzymes were quantified by gel band intensity and normalised to the total protein content.

#### 2.3. Statistical analysis

Samples were taken from both experiments, and individual plants

were considered biological replicates.

Mean values of all parameters of untreated plants of each population are listed in [Suppl. Table 1](#), and possible differences between untreated plants were evaluated using the Student's t-test (significant when  $p \leq 0.05$ ). The same test was used to compare by pairs untreated plants to each dose of glyphosate in each population. Significant differences are highlighted with asterisks.

All statistical analyses were performed using SPSS 27 software. Graphs were constructed using the Sigma Plot 12 software.

### 3. Results

Preliminary studies were performed to determine the range of glyphosate doses to be applied to obtain responses that could facilitate the detection of oxidative stress. Sensitive plants were treated with several doses up to 7FR ([Supplementary Fig. S1](#)). Finally, the final experiments were performed by applying 0.5, 1, 2, and 3FR doses. Leaves of all treated plants remained green and turgid after three days. Nevertheless, all treated S individuals died in less than two weeks after glyphosate application; even the 0.5FR treatment was enough to kill them.

R plants were treated with four different doses, with the highest one in 6FR. Resistant plants were not affected visually at the moment of sampling. Even the 6FR treatment did not result in mortality for R individuals, although some visual effects were detected.

#### 3.1. Shikimate accumulation evidences EPSPS inhibition in treated S plants and not in treated R plants

The accumulation of shikimate in plant tissue can be used to distinguish resistant and sensitive plants. Shikimate accumulation was observed in leaf disk tissue from S plants, evidencing that EPSPS was inhibited ([Fig. 1](#)). The shikimate accumulation was very noticeable in all treated S plants and was maximised when the plants were sprayed with

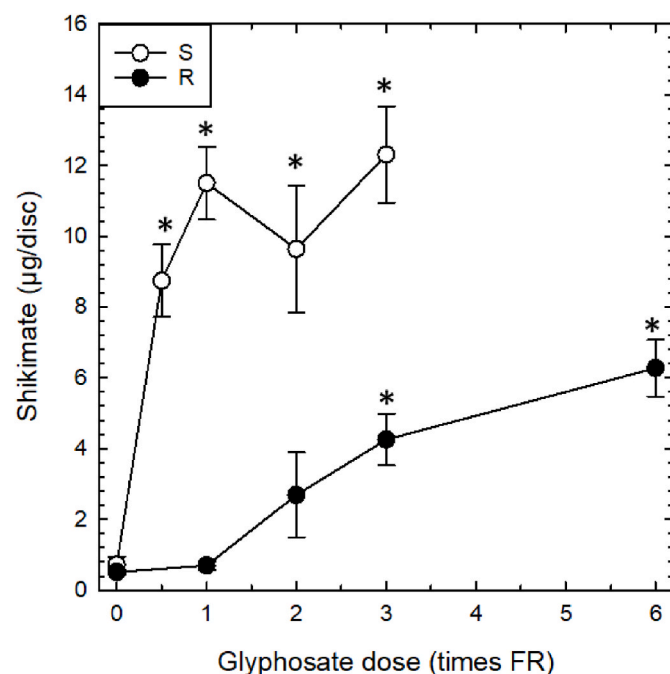


**Fig. 1.** Shikimate content in *Amaranthus palmeri* sensitive (S, white) and resistant (R, black) populations treated with different glyphosate doses (X-axis, times recommended field rate or FR, FR = 0.84 kg ha<sup>-1</sup>). Mean  $\pm$  SE (n = 4–13). Significant differences between treatments and the respective untreated plants of each population are marked with asterisks (Student's t-test, p-value  $\leq 0.05$ ).

FR. Significant shikimate accumulation was observed in the R population only with the highest glyphosate doses (3 and 6FR).

#### 3.2. ROS were accumulated in treated S plants and not in treated R plants

The treated S plants showed significant ROS accumulation. Untreated R plants showed higher H<sub>2</sub>O<sub>2</sub> values than untreated S plants ([Suppl. Table 1](#)), but as shown in [Fig. 2A](#), glyphosate caused a significant increase in H<sub>2</sub>O<sub>2</sub> content in S plants, exceeding 250% of that in untreated plants. The increase was not proportional to glyphosate dose as all treated plants, even those treated with 0.5FR, showed a similar H<sub>2</sub>O<sub>2</sub> content. In terms of the O<sub>2</sub><sup>-</sup> content, the pattern was similar with a significant increase in the former radical in the treated S plants ([Fig. 2B](#)). The pattern of R plants was completely different as both untreated and treated plants showed similar levels of ROS, regardless of the applied dose.

#### 3.3. Small oxidative damage in S plants treated with high glyphosate doses

The S and R plants also responded differently in terms of the oxidative damage caused by glyphosate ([Fig. 3](#)). MDA equivalent content was measured as an indicator of lipid peroxidation. Basal MDA levels were similar in untreated S and R plants; however, in S plants, it increased with the glyphosate dose, reaching a remarkable level in plants treated with 3FR ([Fig. 3A](#)). Basal protein carbonylation level was also similar between untreated S and R plants ([Suppl. Table 1](#)). Nevertheless, carbonyl groups did not change with glyphosate dose in the S plants ([Fig. 3B](#)). Consistent with the results of ROS accumulation, R plants did not suffer oxidative damage to lipids or proteins due to the action of glyphosate.

#### 3.4. General and non-enzymatic antioxidant response

General antioxidant capacity was measured using ABTS and DPPH assays. Both populations showed a similar basal antioxidant capacity and did not vary significantly between treatments, as observed in both the ABTS and DPPH assays ([Fig. 4](#)).

Nonetheless, by delving into the different classes of antioxidants, some significant tendencies were found, such as in the case of glutathione, ascorbate, and related compounds ([Figs. 5 and 6](#)). In the case of glutathione, both reduced (GSH, [Fig. 5A](#)) and oxidised (GSSG, [Fig. 5B](#)) forms increased with the glyphosate dose in the S plants. Therefore, total glutathione content ([Fig. 5E](#)) also increased significantly with glyphosate dose in this population. Cysteine ([Fig. 5C](#)) and  $\gamma$ -glutamyl-cysteine (GGC, the first precursor in the GSH synthesis pathway, [Fig. 5D](#))) showed a pattern similar to glutathione. The GSH-to-GSSG ratio did not vary ([Fig. 5F](#)). The R population showed a very similar basal level to the S population in all these parameters; however, none of these changed significantly with any glyphosate dose (only a slight and non-significant increase in GSSG ([Fig. 5B](#)) and a subsequent decrease in the GSH to GSSG ratio could be detected).

As far as ascorbate is concerned, the pattern of ascorbic acid ([Fig. 6A](#)) and dehydroascorbate ([Fig. 6B](#)) in the S population was almost opposite. A dose-dependent decrease in ascorbic acid was detected ([Fig. 6A](#)), whereas DHA tended to slightly increase with glyphosate dose ([Fig. 6B](#)). Because the majority of ascorbate was in the form of ascorbic acid, the sum of both ascorbate forms ([Fig. 6C](#)) drew a similar pattern to ascorbic acid, and the ascorbic acid/dehydroascorbate ratio ([Fig. 6D](#)) reached very low values with high glyphosate doses owing to the oxidation of the ascorbate pool. R plants showed basal values similar to those of S plants for all four parameters. Contrary to the S population, ascorbic acid and the sum tended to increase with high glyphosate doses, while no appreciable variations were observed in the ascorbic acid/dehydroascorbate ratio.



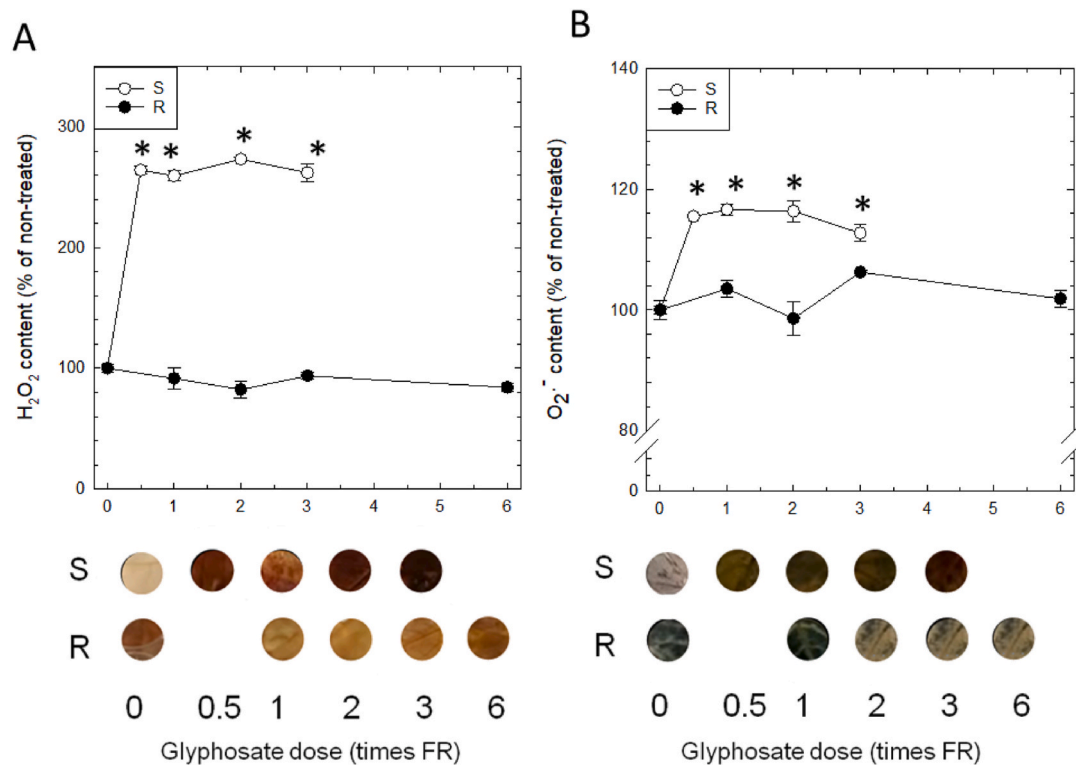


**Fig. 2.** Hydrogen peroxide (A) and superoxide (B) content in *Amaranthus palmeri* sensitive (S, white) and resistant (R, black) populations treated with different glyphosate doses (X-axis, times recommended field rate or FR, FR = 0.84 kg ha<sup>-1</sup>). Mean  $\pm$  SE (n = 3). Significant differences between treatments and the respective untreated plants of each population are marked with asterisks (Student's t-test, p-value  $\leq$  0.05). A representative leaf disk for each population and treatment is shown below.

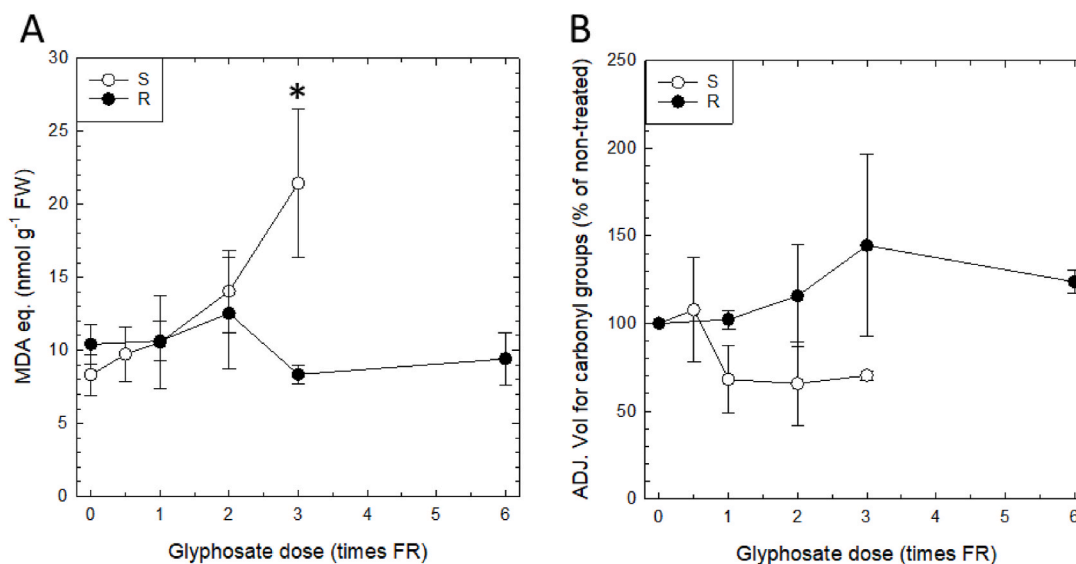


**Fig. 3.** Malondialdehyde (MDA) equivalents (A) and relative intensity of carbonyl groups in membranes (B) in *Amaranthus palmeri* sensitive (S, white) and resistant (R, black) populations treated with different glyphosate doses (X-axis, times recommended field rate or FR, FR = 0.84 kg ha<sup>-1</sup>). Mean  $\pm$  SE (A: n = 4; B: n = 3). Protein carbonyl groups were normalised to the total protein content. Significant differences between treatments and the respective untreated plants of each population are marked with asterisks (Student's t-test, p-value  $\leq$  0.05).

### 3.5. Marginal glyphosate-dependent variations in most antioxidant enzymes

In terms of the enzymatic antioxidant activity, the pattern of each enzyme was different; therefore, no common patterns were detected. However, in general terms, non-significant variations were predominant

(Fig. 7). The basal activities of all enzymes were similar in both populations. CAT activity (Fig. 7A) of the S population decreased transiently with FR but increased again with 2FR and 3FR. POX (Fig. 7B) was the most affected enzyme in the S population, significantly increasing with glyphosate dose. GR activity (Fig. 7C) also tended to increase in the S population, but this increase was very small. None of these three

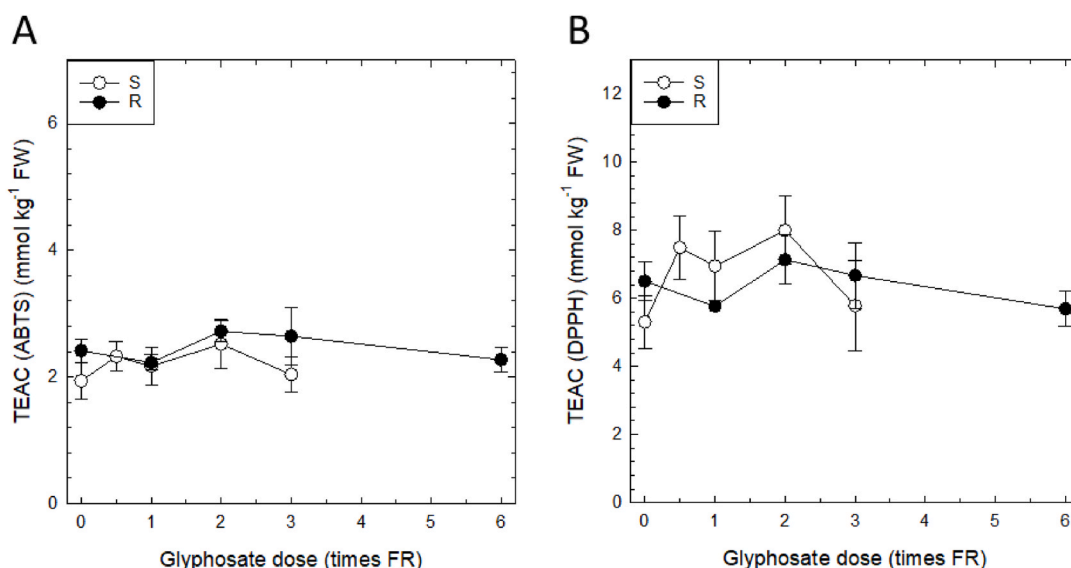


**Fig. 4.** Antioxidant capacity in Trolox Equivalent Antioxidant Capacity (TEAC) determined by ABTS (A) and DPPH (B) methods in *Amaranthus palmeri* sensitive (S, white) and resistant (R, black) populations treated with different glyphosate doses (X-axis, times recommended field rate or FR, FR = 0.84 kg ha<sup>-1</sup>). Mean  $\pm$  SE (n = 4). Trolox equivalents refer to FW.

enzymes showed significant variation for changing glyphosate doses in the R population. APX activity (Fig. 7D) was extremely variable between individuals of both populations.

S plants (treated with 2FR or lower) maintained a similar SOD activity to untreated plants, but it increased in the sample treated with 3FR (Fig. 8); however, there was no variation in the SOD activity in R plants. SOD isoenzymes were characterised in untreated plants and plants treated with FR and 3FR. The three isoenzymes, MnSOD, CuZnSOD1, and CuZnSOD2, did not respond similarly, although in all of them the level in untreated S and R plants was similar (Suppl. Table 1). CuZnSOD2 was the one that increased more in the two populations with FR and 3FR, reaching a relative intensity of 300% of the control in both populations. The patterns of MnSOD and CuZnSOD1 were similar; both increased with 3FR in S plants and decreased with the same dose in R plants. In particular, the decrease in MnSOD was significant, which was the only significant variation in the R population for all the measured parameters. Nevertheless, the variability in relative intensities was high, especially in the S population.

#### 4. Discussion

As observed in other studies, shikimate accumulated more in S than R plants that had received herbicide treatments (Barco-Antoñanzas et al., 2022; Fernández-Escalada et al., 2016), evidencing that R plants overexpressing EPSPS have not completely inhibited EPSPS activity. Consequently, the milder physiological effects of glyphosate in R plants can be related to a lack of inhibition of EPSPS activity.

Accumulating evidence has shown that glyphosate enhances ROS formation in plants (Ahsan et al., 2008; Gomes et al., 2017; Gomes and Juneau, 2016; Zhong et al., 2018) and green algae (Iummato et al., 2019). This study confirmed that H<sub>2</sub>O<sub>2</sub> and superoxide accumulated in the leaves of sensitive plants after five days of glyphosate treatment, and accumulation was not dose-dependent. H<sub>2</sub>O<sub>2</sub> was the ROS that accumulated the most in response to glyphosate. Although the superoxide formation was higher in treated leaves of S plants, it was not as apparent as H<sub>2</sub>O<sub>2</sub> probably due to the biochemical differences between both ROS. Superoxide is a short-lived and locally produced molecule, whereas H<sub>2</sub>O<sub>2</sub> is the most stable ROS, which makes it most prone to accumulation (Demidchik, 2015).

Lipid peroxidation (detected as MDA accumulation) was detected in the S population after the application of the highest dose of glyphosate,

as observed by Maroli et al. (2015) in other two *A. palmeri* populations. In general, lipid peroxidation is a well-known secondary effect of oxidative stress and in the case of the oxidative stress detected after glyphosate it has been described in many other plant species, including maize, soybean, rice, duckweed, and peanuts (Ahsan et al., 2008; Gomes and Juneau, 2016; Iummato et al., 2019; Moldes et al., 2008; Radwan and Fayez, 2016; Sergiev et al., 2006; Soares et al., 2019; Zhong et al., 2018). Protein carbonylation, which is also a classical oxidative damage marker, did not occur after glyphosate treatment in any population. Although glyphosate-induced protein carbonylation has been observed in other species, such as *Arabidopsis thaliana* treated with high glyphosate doses (de Freitas-Silva et al., 2017), it has a much less reported effect than lipid peroxidation. In addition, the effects reported by de Freitas-Silva et al. (2017) were observed 14 days after glyphosate treatment (3 days in the current study). The lack of protein carbonylation and the dose-dependency of MDA indicated that the moderate oxidative damage was not the cause of plant death after glyphosate exposure, as 0.5FR was sufficient to kill all S plants; however, a much higher dose was necessary to induce significant MDA accumulation.

In S plants, glutathione is synthesised in a larger quantity proportional to the glyphosate dose. Glyphosate-induced accumulation or enhanced synthesis of GSH has also been reported in other plant species and green algae, such as peas, peanuts, and *Arabidopsis thaliana* (de Freitas-Silva et al., 2017; Iummato et al., 2019; Jain and Bhalla-Sarin, 2000; Miteva et al., 2010; Romero et al., 2011; Sergiev et al., 2006; Zulet et al., 2015). Vivancos et al. (2011) analysed the glutathione status in glyphosate-sensitive and glyphosate-resistant soybean and found that GSH synthesis was only enhanced in the sensitive samples, despite the significant glyphosate accumulation in resistant samples. This suggests that the effect on GSH homeostasis is modulated in response to glyphosate-dependent alterations in the shikimate pathway and amino acid metabolism and is not due to the mere presence of glyphosate. Our results corroborate this trend in *A. palmeri*, showing an accumulation of glutathione forms and the precursors in the biosynthetic pathway (Cys and GGC) in S plants and no significant changes in R plants.

The content of ascorbic acid decreased with glyphosate treatment in S plants, contrary to the effect detected in glutathione. According to Gomes et al. (2017), a reduction in the ascorbate pool in treated plants may be due to a reduced electron transport rate that results from photosynthetic damage caused by glyphosate. The dehydroascorbate content, however, showed a slight upward trend, which probably means

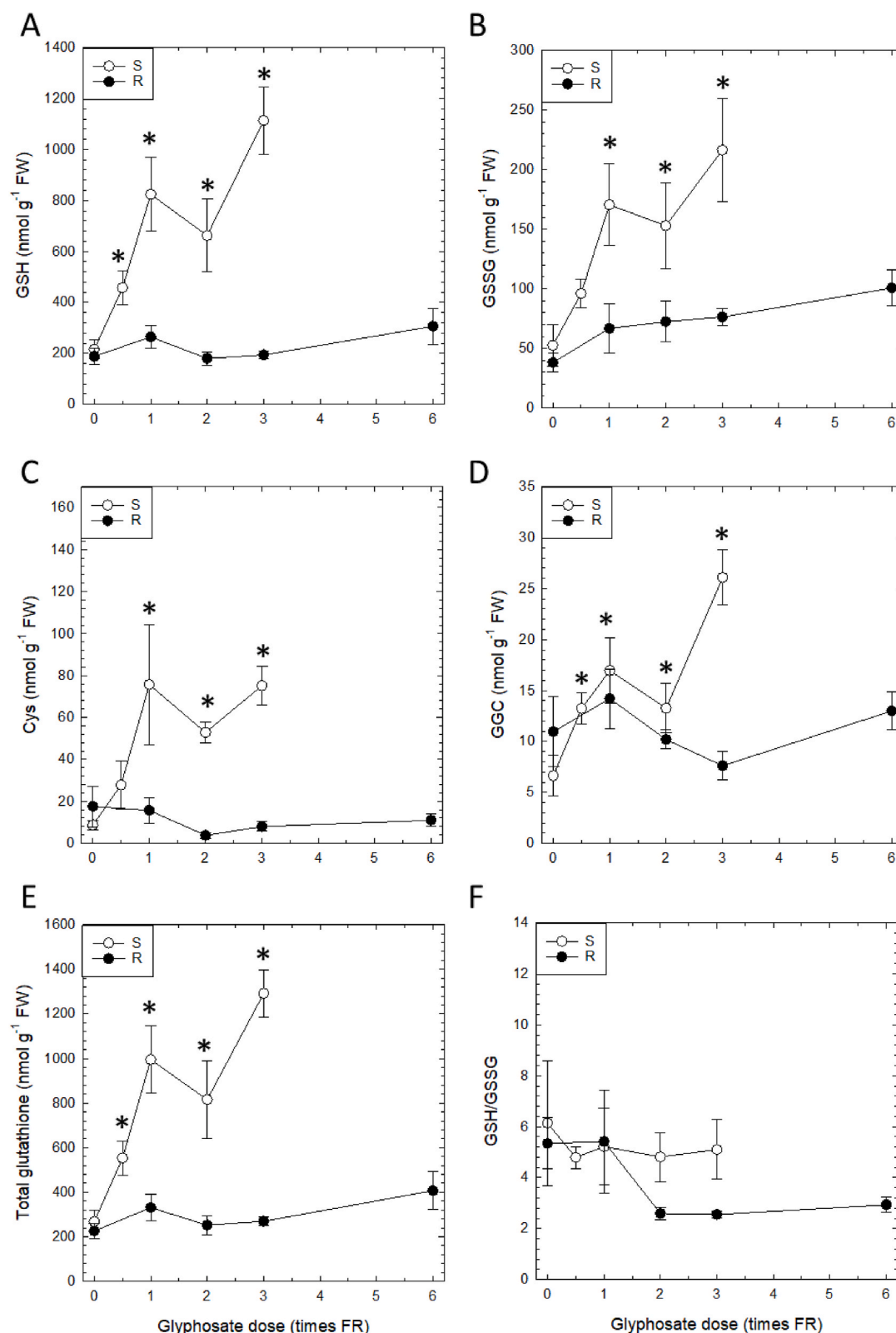


**Fig. 5.** Glutathione-related data in *Amaranthus palmeri* sensitive (S, white) and resistant (R, black) populations treated with different glyphosate doses (X-axis, times recommended field rate or FR, FR = 0.84 kg ha<sup>-1</sup>): reduced glutathione (GSH) content (A), oxidised glutathione (GSSG) content (B), cysteine (Cys) content (C),  $\gamma$ -glutamyl-cysteine (GGC) content (D), total glutathione content (E) and GSH/GSSG ratio (F). Mean  $\pm$  SE (n = 4). Significant differences between treatments and the respective untreated plants of each population are marked with asterisks (Student's t-test, p-value  $\leq 0.05$ ).

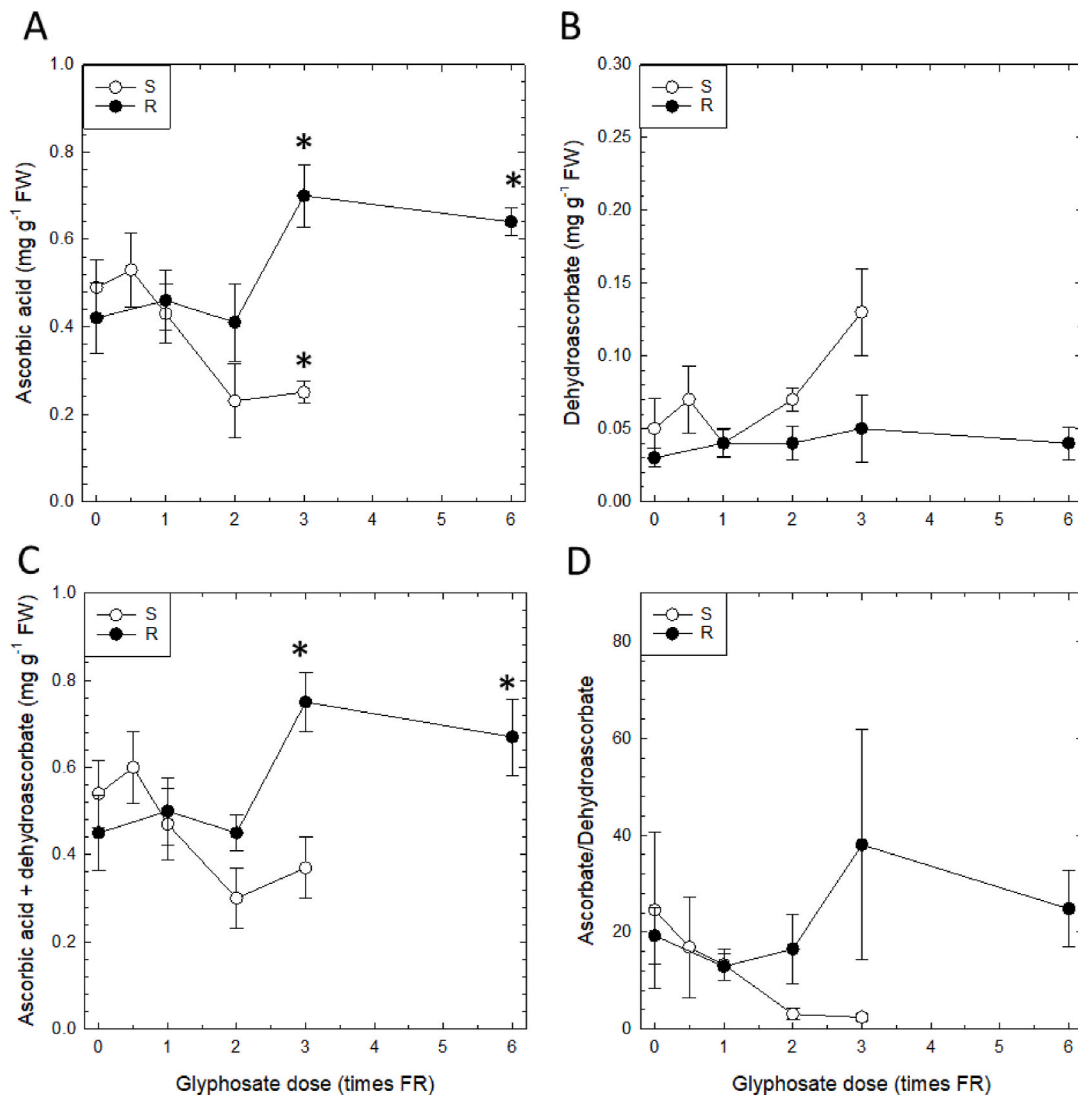


**Fig. 6.** Ascorbate-related data in *Amaranthus palmeri* sensitive (S, white) and resistant (R, black) populations treated with different glyphosate doses (X-axis, times recommended field rate or FR, FR = 0.84 kg ha<sup>-1</sup>): ascorbic acid content (A), dehydroascorbate content (B), the sum of ascorbic acid and dehydroascorbate contents (C) and ascorbic acid to dehydroascorbate ratio (D). Mean  $\pm$  SE (n = 4). Significant differences between treatments and the respective untreated plants of each population are marked with asterisks (Student's t-test, p-value  $\leq$  0.05).

that ascorbic acid was partially oxidised to dehydroascorbate. These changes in glutathione and ascorbate levels show that glyphosate disrupts the redox balance of the ascorbate-glutathione pathway in S plants, an unmistakable sign of oxidative stress. In R plants, the ascorbic acid pool (and thus, the sum of ascorbic acid and dehydroascorbate) increased with the highest glyphosate dose. This indicates that glyphosate induces minimal antioxidant activation in resistant plants. The importance of this result is questionable given the absence of oxidative damage and inconsiderable variations in antioxidant capacity and glutathione metabolism.

In the present study, alterations in non-enzymatic antioxidants were generally not accompanied by major increases in enzymatic activities. Despite the changes in glutathione and ascorbate in the S population, GR and APX activities (two of the main enzymes of the ascorbate-glutathione pathway) did not change. Previous studies on CAT have shown inconsistent results, with its glyphosate-dependent variations increasing (Hernández-García and Martínez-Jerónimo, 2020; Kielak et al., 2011), not changing (Ke et al., 2021), or decreasing (da Silva Santos et al., 2020; Iummato et al., 2019; Yu et al., 2021). In the current study, the SOD activity did not vary significantly with glyphosate dose in the S population; however, it tended to increase with the highest dose,

and there were no changes in the R population. A characterisation assay revealed that CuZnSOD2 contributed the most to this pattern in the S population. Both MnSOD and CuZnSOD1 increased in S plants treated with 3 FR, and FR was sufficient to observe a CuZnSOD2 increase; however, these increases were not significant. The fact that SOD can be inactivated by H<sub>2</sub>O<sub>2</sub> (Kronberg et al., 2021) could explain why SOD activity increases only slightly despite superoxide accumulation. Although all SOD isoenzymes have similar functions and affinities, MnSOD is mitochondria-based; meanwhile, CuZnSOD is present in the cytosol and many cellular locations, such as chloroplasts (Kim et al., 2010; Stephenie et al., 2020), which may be the cause of the lower responsiveness of MnSOD.

Thus, the only enzymatic activity that increased in response to glyphosate in the S population was POX, an effect already observed in other studies (Moldes et al., 2008). Peroxidases are a vast group of enzymes that, among other functions, act as H<sub>2</sub>O<sub>2</sub> scavengers and their activity can increase because of membrane lipid peroxidation (Radwan and Fayed, 2016). Although this would explain the similarities between lipid peroxidation and POX activity, it would not explain why it was the only activated enzymatic activity. Peroxidases have many functions apart from those of antioxidants, which might be responsible for changes



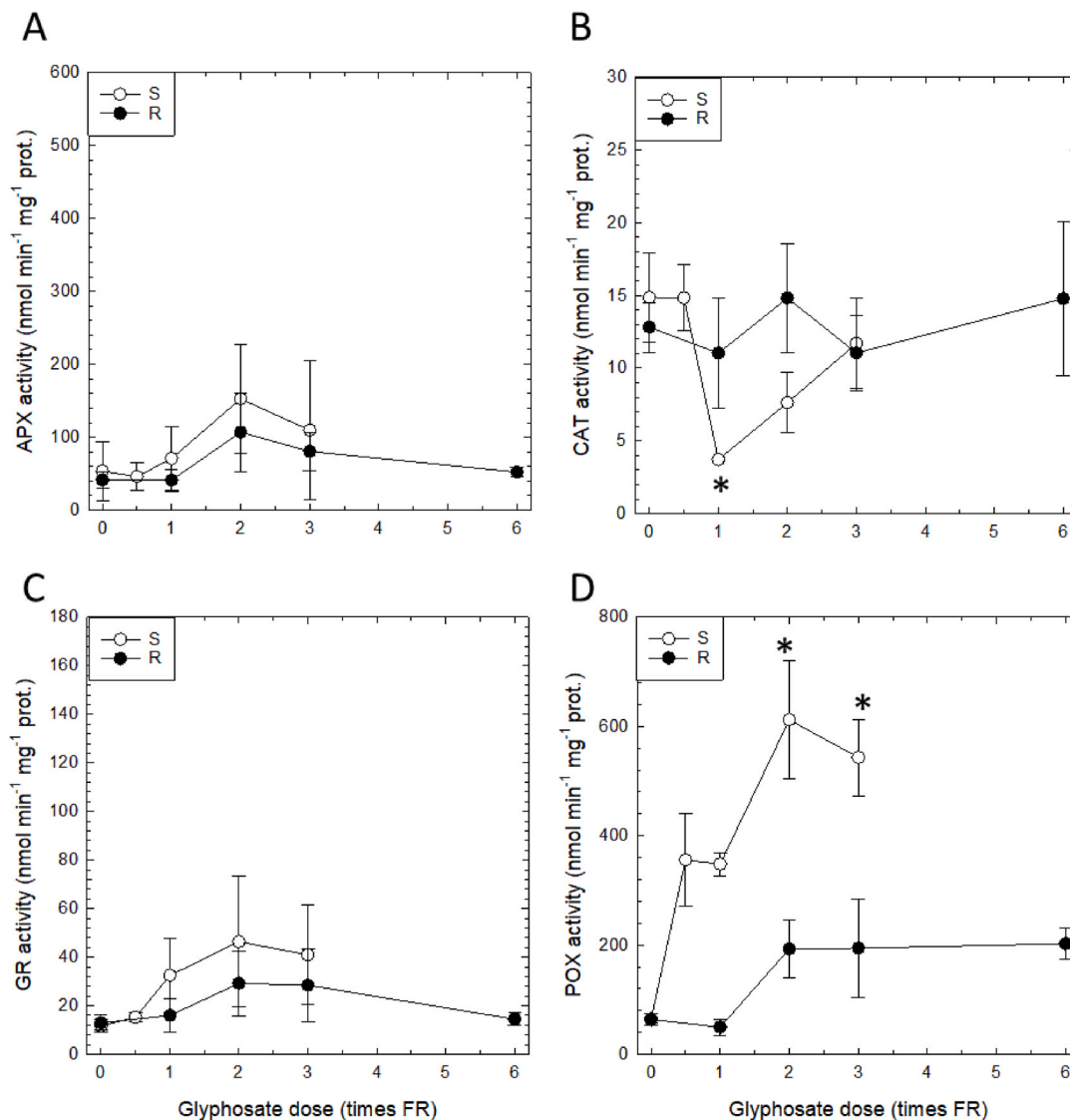


**Fig. 7.** Different antioxidant enzymes (ascorbate peroxidase (APX) (A), catalase (CAT) (B), glutathione reductase (GR) (C), and peroxidases (POX) (D)) activity in *Amaranthus palmeri* sensitive (S, white) and resistant (R, black) populations treated with different glyphosate doses (X-axis, times recommended field rate or FR, FR = 0.84 kg ha<sup>-1</sup>). Mean  $\pm$  SE (n = 4). Significant differences between treatments and the respective untreated plants of each population are marked with asterisks (Student's t-test, p-value  $\leq$  0.05).

in POX activity under different circumstances. In this case, the increase in POX activity could be linked to glyphosate-induced changes in the phenolic metabolism, which consist of an increase in the amount of benzoic acid and other soluble hydroxyphenolics, which is directly induced by shikimate pathway disruption (Cañal et al., 1987). Moreover, in the plant defence mechanisms modulated by glyphosate lipid peroxidation and plant defense-related phytohormones are affected (Fuchs et al., 2021). Besides that, it cannot be discarded that the increase of oxidative stress markers in S plants could be related to the inhibition of biosynthesis of several phenolic antioxidants derived from the shikimate pathway (Hoagland, 1980).

A clear oxidative stress was detected in the S plants treated with the highest dose of glyphosate, as evident by lipid peroxidation and the oxidised ascorbate pool. The induction of the activity of the antioxidant enzymes SOD or GSH was not sufficient to prevent oxidative damage in S plants. However, there are some stress markers apart from oxidative stress and other physiological effects attributed to glyphosate in other plant species, such as ethylene accumulation (Lee and Dumas, 1983), decreased auxin levels (Jain and Bhalla-Sarin, 2001; Lee and Dumas, 1983), and cyanotoxin production (Hernández-García and

Martínez-Jerónimo, 2020). Indeed, glutathione production may be related to multiple detoxification functions (de Freitas-Silva et al., 2017). Therefore, the increase in GSH content may be a response to glyphosate toxicity triggered by a blockade of the shikimate pathway (Jain and Bhalla-Sarin, 2001), although it acts as a redox buffer and H<sub>2</sub>O<sub>2</sub> scavenger. There may be different immediate causes for the increase in the GSH content. One of them could be a decrease in the levels of auxin (Lee and Dumas, 1983) and porphyrin-containing enzymes caused by the action of glyphosate (Jain and Bhalla-Sarin, 2001). It may also enhance glutathione S-transferase (GST) activity, an enzyme that detoxifies xenobiotics by catalysing the conjugation of GSH, and its activity has been reported to increase in response to glyphosate (Ahsan et al., 2008; Chen et al., 2017; Jain and Bhalla-Sarin, 2001; Miteva et al., 2010; Sergiev et al., 2006). A significant increase in the amino acid pool in treated S plants may also be responsible for the enhanced glutathione synthesis. Indeed, all glutathione precursors accumulated after glyphosate accumulation in both *A. palmeri* (Fig. 4) and *Pisum sativum* (Zulet et al., 2015). Unlike glutathione synthesis, oxidation and subsequent GSSG formation are an effect of ROS accumulation.

Unlike treated plants in the S population, treated R plants did not die,

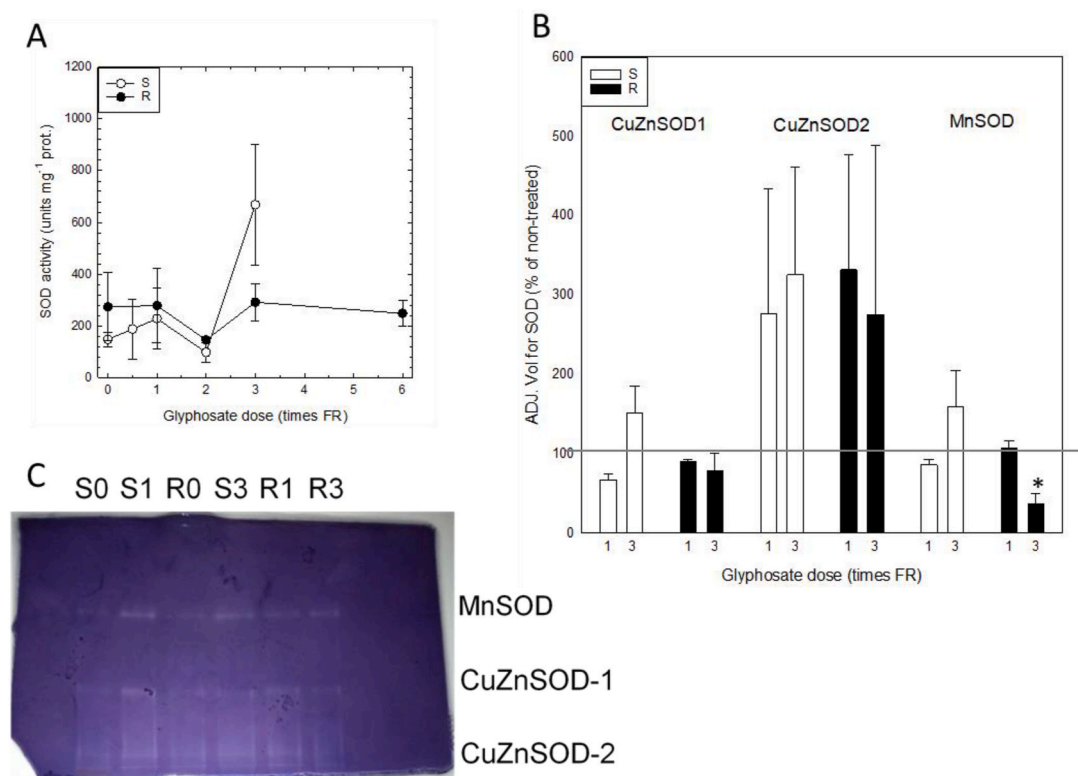


**Fig. 8.** SOD activity (A) and relative intensity in gels of different SOD isoenzymes (B) in *Amaranthus palmeri* sensitive (S, white) and resistant (R, black) populations treated with different glyphosate doses (X-axis, times recommended field rate or FR, FR = 0.84 kg ha<sup>-1</sup>). Mean  $\pm$  SE (A: n = 4; B: n = 6). Significant differences between treatments and the respective untreated plants of each population are marked with asterisks (Student's t-test, p-value  $\leq$  0.05). A representative gel is shown (C).

accumulate shikimate (to the same extent as S plants), accumulate ROS, or suffer oxidative damage. This confirms that EPSPS overexpression not only protects resistant *A. palmeri* plants from shikimate pathway disruption caused by glyphosate, but also from the induced oxidative stress that was detected in S plants after EPSPS inhibition. This implies that oxidative stress caused by glyphosate in *A. palmeri* is related to EPSPS inhibition and shikimate pathway blocking, as suggested by Ahsan et al. (2008) and Sergiev et al. (2006) for maize and rice, respectively. Furthermore, the similarity in terms of the antioxidant pool between untreated S and R plants of this study indicated that EPSPS overexpression is not accompanied by an increased tolerance to oxidative stress. On the contrary (Maroli et al., 2015), described another *A. palmeri* biotype where glyphosate resistance due to EPSPS overexpression was complemented by antioxidant systems.

Although several studies have demonstrated that glyphosate induces oxidative stress in plants, the exact mechanism by which ROS are generated remains unknown. Typical ROS sources in stressed plants include the electron transport chain (ETC) of chloroplasts and mitochondria (Demidchik, 2015), NADH/NADPH-dependent ETC, and xanthine oxidase in peroxisomes (del Río et al., 2006). Gomes and Juneau (2016) performed confocal evaluations for duckweed and revealed that ROS are initially produced outside of the chloroplast upon glyphosate exposure, and thus proposed mitochondrial ETC as a potential target of glyphosate and the possible origin of H<sub>2</sub>O<sub>2</sub>. Additionally, POX activity is a possible source of ROS. Peroxidases generate superoxide anions and can either detoxify or generate H<sub>2</sub>O<sub>2</sub> (Martínez et al., 1998; Mika et al., 2010), indicating that increased POX activity may be responsible for ROS generation. This hypothesis is reinforced by the similarities between ROS content and POX data, both of which are high in treated S plants. As explained before, the increase in POX activity is presumably due to factors other than ROS accumulation, indicating that this group of enzymes probably acts as a ROS source rather than a

scavenger. Superoxide generation due to increased POX activity has been demonstrated to be a central mechanism for various abiotic and biotic stresses (Chang et al., 2012; Demidchik, 2015; Steffens et al., 2013).

Shikimate accumulation indicates EPSPS inhibition in S plants, and a clear oxidative stress was detected. ROS accumulation and oxidative stress barely occur in R plants, which show only a moderate increase in POX activity at an extremely high glyphosate dose, when EPSPS was affected, as indicated by shikimate accumulation. These results indicate that oxidative stress is related to EPSPS and it is prevented in R plants overexpressing EPSPS. However, the exact mechanisms linking oxidative stress and EPSPS inhibition remain unclear. Some other physiological aspects of the mode of action of glyphosate would lead to oxidative stress, such as the content of metabolites derived from the shikimate pathway (phenylpropanoids, anthocyanines).

## 5. Conclusion

In summary, the data obtained in this study demonstrate that glyphosate causes secondary physiological effects in *A. palmeri*, beyond the direct effects of shikimate pathway disruption. One of these effects is mild oxidative stress, which has demonstrated to be a secondary effect of EPSPS inhibition, as plants overexpressing the enzyme do not show changes in the oxidative markers. The oxidative stress manifested in lipid peroxidation and changes in the antioxidant pool in the sensitive population were probably related to the ROS production due to POX activity, which in turn is related to EPSPS inhibition. Further research on the physiological mechanisms linking POX activity with EPSPS inhibition is needed to confirm this hypothesis. Some lethal doses did not induce major oxidative damage, even in the sensitive population, indicating that glyphosate toxicity is independent of induced oxidative stress.

## CRediT authorship contribution statement

**Mikel Vicente Eceiza:** Methodology, Investigation, Formal analysis, Writing – original draft, Writing – review & editing. **Miriam Gil-Monreal:** Validation, Formal analysis, Writing – review & editing. **María Barco-Antoñanzas:** Methodology, Writing – review & editing. **Ana Zabalza:** Conceptualization, Writing – original draft, Writing – review & editing, Resources. **Mercedes Royuela:** Conceptualization, Writing – review & editing, Resources, Visualization, All authors have read and agreed to the published version of the manuscript.

## Declaration of competing interest

The authors declare that they have no known competing financial interests or personal relationships that could have appeared to influence the work reported in this paper.

## Acknowledgments

The authors would like to acknowledge G. Garijo and J. Encinas for technical assistance. T. Gaines (Colorado State University, CO, USA) is acknowledged for providing seeds. This work was funded by the Spanish Ministry of Economy and Competitiveness (AGL2016-77531-R), the Public University of Navarre (Project UPNA20-6138) and the Spanish Ministry of Science and Innovation (2020 117723-RB-100). M.V. Eceiza is the holder of a predoctoral fellowship of the Basque Government. Open access funding provided by Universidad Pública de Navarra.

## Appendix A. Supplementary data

Supplementary data to this article can be found online at <https://doi.org/10.1016/j.jplph.2022.153720>.

## References

- Ahsan, N., Lee, D.G., Lee, K.W., Alam, I., Lee, S.H., Bahk, J.D., Lee, B.H., 2008. Glyphosate-induced oxidative stress in rice leaves revealed by proteomic approach. *Plant Physiol. Biochem.* 46, 1062–1070. <https://doi.org/10.1016/j.plaphy.2008.07.002>.
- Arnao, M.B., Cano, A., Acosta, M., 2001. The hydrophilic and lipophilic contribution to total antioxidant activity. *Food Chem.* 73, 239–244. [https://doi.org/10.1016/S0308-8146\(00\)00324-1](https://doi.org/10.1016/S0308-8146(00)00324-1).
- Barco-Antoñanzas, M., Gil-Monreal, M., Eceiza, M.V., Royuela, M., Zabalza, A., 2022. Primary metabolism in an *Amaranthus palmeri* population with multiple resistance to glyphosate and pyriithiobac herbicides. *Plant Sci.* 318, 111212 <https://doi.org/10.1016/j.plantsci.2022.111212>.
- Beauchamp, C., Fridovich, I., 1971. Superoxide dismutase: improved assays and an assay applicable to acrylamide gels. *Anal. Biochem.* 44, 276–287. [https://doi.org/10.1016/0003-2697\(71\)90370-8](https://doi.org/10.1016/0003-2697(71)90370-8).
- Bradford, M., 1976. A rapid and sensitive method for the quantitation of microgram quantities of protein utilizing the principle of protein-dye binding. *Anal. Biochem.* 72, 248–254. <https://doi.org/10.1006/abio.1976.9999>.
- Brand-Williams, W., Cuvelier, M.E., Berset, C., 1995. Use of a free radical method to evaluate antioxidant activity. *LWT - Food Sci. Technol. (Lebensmittel-Wissenschaft - Technol.)* 28, 25–30. [https://doi.org/10.1016/S0023-6438\(95\)80008-5](https://doi.org/10.1016/S0023-6438(95)80008-5).
- Bridges, S.M., Salin, M.L., 1981. Distribution of iron-containing superoxide dismutase in vascular plants. *Plant Physiol.* 68, 275–278. <https://doi.org/10.1104/pp.68.2.275>.
- Cañal, M.J., Sánchez-Tamés, R., Fernández, B., 1987. Effects of glyphosate on phenolic metabolism in yellow nutsedge leaves. *Physiol. Plantarum* 69, 627–632. <https://doi.org/10.1111/j.1399-3054.1987.tb01976.x>.
- Caverzan, A., Piasecki, C., Chavarria, G., Stewart, C., Vargas, L., 2019. Defenses against ROS in crops and weeds: the effects of interference and herbicides. *Int. J. Mol. Sci.* 20, 1086. <https://doi.org/10.3390/ijms20051086>.
- Chang, M.L., Chen, N.Y., Liao, L.J., Cho, C.L., Liu, Z.H., 2012. Effect of cadmium on peroxidase isozyme activity in roots of two *Oryza sativa* cultivars. *Bot. Stud.* 53, 31–44.
- Chen, J., Huang, H., Wei, S., Huang, Z., Wang, X., Zhang, C., 2017. Investigating the mechanisms of glyphosate resistance in goosegrass (*Eleusine indica* (L.) Gaertn.) by RNA sequencing technology. *Plant J.* 89, 407–415. <https://doi.org/10.1111/tpl.13395>.
- Corpas, F.J., Barroso, J.B., Sandalio, L.M., Distefano, S., Palma, J.M., Lupiáñez, J.A., Del Río, L.A., 1998. A dehydrogenase-mediated recycling system of NADPH in plant peroxisomes. *Biochem. J.* 330, 777–784. <https://doi.org/10.1042/bj3300777>.
- Culpepper, A.S., Grey, T.L., Vencill, W.K., Kichler, J.M., Webster, T.M., Brown, S.M., York, A.C., Davis, J.W., Hanna, W.W., 2006. Glyphosate-resistant Palmer amaranth (*Amaranthus palmeri*) confirmed in Georgia. *Weed Sci.* 54, 620–626. <https://doi.org/10.1614/WS-06-001R.1>.
- da Silva Santos, J., da Silva Pontes, M., Grillo, R., Fiorucci, A.R., Arruda, G.J., Santiago, E.F., 2020. Physiological mechanisms and phytoremediation potential of the macrophyte *Salvinia biloba* towards a commercial formulation and an analytical standard of glyphosate. *Chemosphere* 259. <https://doi.org/10.1016/j.chemosphere.2020.127417>.
- Daudi, A., O'Brien, J.A., 2012. Detection of hydrogen peroxide by DAB staining in Arabidopsis leaves. *Bio-Protocol* 2, e263. <https://doi.org/10.21769/BioProtoc.263>.
- de Freitas-Silva, L., Rodríguez-Ruiz, M., Houmani, H., da Silva, L.C., Palma, J.M., Corpas, F.J., 2017. Glyphosate-induced oxidative stress in *Arabidopsis thaliana* affecting peroxisomal metabolism and triggers activity in the oxidative phase of the pentose phosphate pathway (OxPPP) involved in NADPH generation. *J. Plant Physiol.* 218, 196–205. <https://doi.org/10.1016/j.jplph.2017.08.007>.
- del Río, L.A., Sandalio, L.M., Corpas, F.J., Palma, J.M., Barroso, J.B., 2006. Reactive oxygen species and reactive nitrogen species in peroxisomes. Production, scavenging, and role in cell signaling. *Plant Physiol.* 141, 330–335. <https://doi.org/10.1104/pp.106.078204>.
- Demidchik, V., 2015. Mechanisms of oxidative stress in plants: from classical chemistry to cell biology. *Environ. Exp. Bot.* 109, 212–228. <https://doi.org/10.1016/j.envexpbot.2014.06.021>.
- Dogramaci, M., Anderson, J.V., Chao, W.S., Horvath, D.P., Hernandez, A.G., Mikel, M.A., Foley, M.E., 2017. Foliar glyphosate treatment alters transcript and hormone profiles in crown buds of leafy spurge and induces dwarfed and bushy phenotypes throughout its perennial lifecycle. *Plant Genome* 10, 1–23. <https://doi.org/10.3835/plantgenome2016.09.0098>.
- Duke, S.O., 2018. The history and current status of glyphosate. *Pest Manag. Sci.* 74, 1027–1034. <https://doi.org/10.1002/ps.4652>.
- Edwards, R., Hannah, M., 2014. Focus on weed control. *Plant Physiol.* 166, 1087–1089. <https://doi.org/10.1104/pp.114.900496>.
- Einhardt, A.M., Ferreira, S., Oliveira, L.M., Ribeiro, D.M., Rodrigues, F.A., 2020. Glyphosate and nickel differently affect photosynthesis and ethylene in glyphosate-resistant soybean plants infected by *Phakopsora pachyrhizi*. *Physiol. Plantarum* 170, 592–606. <https://doi.org/10.1111/ppl.13195>.
- Fernández-Escalada, M., Gil-Monreal, M., Zabalza, A., Royuela, M., 2016. Characterization of the *Amaranthus palmeri* physiological response to glyphosate in susceptible and resistant populations. *J. Agric. Food Chem.* 64, 95–106. <https://doi.org/10.1021/acs.jafc.5b04916>.
- Fernández-Escalada, M., Zulet-González, A., Gil-Monreal, M., Zabalza, A., Ravet, K., Gaines, T., Royuela, M., 2017. Effects of EPSPS copy number variation (CNV) and glyphosate application on the aromatic and branched chain amino acid synthesis pathways in *Amaranthus palmeri*. *Front. Plant Sci.* 8, 1970. <https://doi.org/10.3389/fpls.2017.01970>.
- Fernández-Escalada, M., Zulet-González, A., Gil-Monreal, M., Royuela, M., Zabalza, A., 2019. Physiological performance of glyphosate and imazamox mixtures on *Amaranthus palmeri* sensitive and resistant to glyphosate. *Sci. Rep.* 9, 18225 <https://doi.org/10.1038/s41598-019-54642-9>.
- Fuchs, B., Saikkonen, K., Helander, M., 2021. Glyphosate-modulated biosynthesis driving plant defense and species interactions. *Trends Plant Sci.* 26, 312–323. <https://doi.org/10.1016/j.tplants.2020.11.004>.
- Gaines, T.A., Zhang, W., Wang, D., Bukun, B., Chisholm, S.T., Shaner, D.L., Nissen, S.J., Patzoldt, W.L., Tranel, P.J., Culpepper, A.S., Grey, T.L., Webster, T.M., Vencill, W.K., Sammons, R.D., Jiang, J., Preston, C., Leach, J.E., Westra, P., 2010. Gene amplification confers glyphosate resistance in *Amaranthus palmeri*. *Proc. Natl. Acad. Sci. Unit. States Am.* 107, 1029–1034. <https://doi.org/10.1073/pnas.0906649107>.
- Gaines, T.A., Patterson, E.L., Neve, P., 2019. Molecular mechanisms of adaptive evolution revealed by global selection for glyphosate resistance. *New Phytol.* 223, 1770–1775. <https://doi.org/10.1111/nph.15858>.
- Gomes, M.P., Juneau, P., 2016. Oxidative stress in duckweed (*Lemna minor* L.) induced by glyphosate: is the mitochondrial electron transport chain a target of this herbicide? *Environ. Pollut.* 218, 402–409. <https://doi.org/10.1016/j.envpol.2016.07.019>.
- Gomes, M.P., Smedbol, E., Chalifour, A., Hénault-ethier, L., Labrecque, M., Lepage, L., Lucotte, M., Juneau, P., 2014. Alteration of plant physiology by glyphosate and its by-product aminomethylphosphonic acid: an overview. *J. Exp. Bot.* 65, 4691–4703. <https://doi.org/10.1093/jxb/eru269>.
- Gomes, M.P., Le Manac'h, S.G., Hénault-Ethier, L., Labrecque, M., Lucotte, M., Juneau, P., 2017. Glyphosate-dependent inhibition of photosynthesis in willow. *Front. Plant Sci.* 8, 1–13. <https://doi.org/10.3389/fpls.2017.00207>.
- Heap, I., 2022. The international survey of herbicide resistant weeds. Online. Internet. [WWW Document]. URL <http://www.weeds-science.com/Home.aspx>, 7.8.21.
- Hernández-García, C.I., Martínez-Jerónimo, F., 2020. Multistressor negative effects on an experimental phytoplankton community. The case of glyphosate and one toxigenic cyanobacterium on Chlorophyceae microalgae. *Sci. Total Environ.* 717, 137186 <https://doi.org/10.1016/j.scitotenv.2020.137186>.
- Herrero-Martínez, J.M., Simó-Alfonso, E.F., Ramis-Ramos, G., Deltoro, V.I., Calatayud, A., Barreno, E., 2000. Simultaneous determination of L-ascorbic acid, glutathione, and their oxidized forms in ozone-exposed vascular plants by capillary zone electrophoresis. *Environ. Sci. Technol.* 34, 1331–1336. <https://doi.org/10.1021/es991068l>.
- Hoagland, D.R., Arnon, D.I., 1950. The water-culture method for growing plants without soil. *Calif. Agric. Ext. Serv. Circ.* 347, 1–32. <http://www.cabdirect.org/abstract/s/19500302257.html>.
- Hoagland, R.E., 1980. Effects of glyphosate on metabolism of phenolic compounds: VI. Effects of glyphosine and glyphosate metabolites on phenylalanine ammonia-lyase activity, growth and protein, chlorophyll and anthocyanin levels in soybean (*Glycine*

- max) seedlings. *Weed Sci.* 28, 393–400. <https://doi.org/10.1017/S0043174500055545>.
- Hodges, D.M., DeLong, J.M., Forney, C.F., Prange, R.K., 1999. Improving the thiobarbituric acid-reactive-substances assay for estimating lipid peroxidation in plant tissues containing anthocyanin and other interfering compounds. *Planta* 207, 604–611. <https://doi.org/10.1007/s004250050524>.
- Iummato, M.M., Fassiano, A., Graziano, M., dos Santos Afonso, M., Ríos de Molina, M.C., Juárez, Á.B., 2019. Effect of glyphosate on the growth, morphology, ultrastructure and metabolism of *Scenedesmus vacuolatus*. *Ecotoxicol. Environ. Saf.* 172, 471–479. <https://doi.org/10.1016/j.ecoenv.2019.01.083>.
- Jain, M., Bhalla-Sarin, N., 2000. Effect of glyphosate on the activity of DAHP synthase isozymes in callus cultures of groundnut (*Arachis hypogaea* L.) selected in vitro. *Indian J. Biochem. Biophys.* 37, 235–240.
- Jain, M., Bhalla-Sarin, N., 2001. Glyphosate-induced increase in glutathione S-transferase activity and glutathione content in groundnut (*Arachis hypogaea* L.). *Pestic. Biochem. Physiol.* 69, 143–152. <https://doi.org/10.1006/pest.2000.2535>.
- Jiang, L.X., Jin, L.G., Guo, Y., Tao, B., Qiu, L.J., 2013. Glyphosate effects on the gene expression of the apical bud in soybean (*Glycine max*). *Biochem. Biophys. Res. Commun.* 437, 544–549. <https://doi.org/10.1016/j.bbrc.2013.06.112>.
- Ke, M., Ye, Y., Zhang, Z., Gillings, M., Qu, Q., Xu, N., Xu, L., Lu, T., Wang, J., Qian, H., 2021. Synergistic effects of glyphosate and multiwall carbon nanotubes on *Arabidopsis thaliana* physiology and metabolism. *Sci. Total Environ.* 769, 145156. <https://doi.org/10.1016/j.scitotenv.2021.145156>.
- Kielak, E., Sempuch, C., Mioduszevska, H., Kloczek, J., Leszczyński, B., 2011. Phytotoxicity of Roundup Ultra 360 SL in aquatic ecosystems: biochemical evaluation with duckweed (*Lemna minor* L.) as a model plant. *Pestic. Biochem. Physiol.* 99, 237–243. <https://doi.org/10.1016/j.pestbp.2011.01.002>.
- Kim, M.D., Kim, Y.H., Kwon, S.Y., Yun, D.J., Kwak, S.S., Lee, H.S., 2010. Enhanced tolerance to methyl viologen-induced oxidative stress and high temperature in transgenic potato plants overexpressing the CuZnSOD, APX and NDK2 genes. *Physiol. Plantarum* 140, 153–162. <https://doi.org/10.1111/j.1399-3054.2010.01392.x>.
- Kronberg, M.F., Rossen, A., Munarriz, E.R., 2021. Glyphosate-based herbicides and oxidative stress. In: Patel, V.B., Preedy, V.R. (Eds.), *Toxicology*. Academic Press, pp. 79–90. <https://doi.org/10.1016/b978-0-12-819092-0.00009-1>.
- Labhili, M., Joudrier, P., Gautier, M.F., 1995. Characterization of cDNAs encoding *Triticum durum* dehydrins and their expression patterns in cultivars that differ in drought tolerance. *Plant Sci.* 112, 219–230. [https://doi.org/10.1016/0168-9452\(95\)04267-9](https://doi.org/10.1016/0168-9452(95)04267-9).
- Lee, T.T., Dumas, T., 1983. Effect of glyphosate on ethylene production in tobacco callus. *Plant Physiol.* 72, 855–857. <https://doi.org/10.1104/pp.72.3.855>.
- Maroli, A.S., Nandula, V.K., Dayan, F.E., Duke, S.O., Gerard, P., Tharayil, N., 2015. Metabolic profiling and enzyme analyses indicate a potential role of antioxidant systems in complementing glyphosate resistance in an *Amaranthus palmeri* biotype. *J. Agric. Food Chem.* 63, 9199–9209. <https://doi.org/10.1021/acs.jafc.5b04223>.
- Martinez, C., Montillet, J.L., Bresson, E., Agnel, J.P., Dai, G.H., Daniel, J.F., Geiger, J.P., Nicole, M., 1998. Apoplastic peroxidase generates superoxide anions in cells of cotton cotyledons undergoing the hypersensitive reaction to *Xanthomonas campestris* pv. *malvacearum* race 18. *Mol. Plant Microbe Interact.* 11, 1038–1047. <https://doi.org/10.1094/MPMI.1998.11.11.1038>.
- Mika, A., Boenisch, M.J., Hopff, D., Lühje, S., 2010. Membrane-bound guaiacol peroxidases from maize (*Zea mays* L.) roots are regulated by methyl jasmonate, salicylic acid, and pathogen elicitors. *J. Exp. Bot.* 61, 831–841. <https://doi.org/10.1093/jxb/erp353>.
- Miteva, L.P.E., Ivanov, S.V., Alexieva, V.S., 2010. Alterations in glutathione pool and some related enzymes in leaves and roots of pea plants treated with the herbicide glyphosate. *Russ. J. Plant Physiol.* 57, 131–136. <https://doi.org/10.1134/S1021443710010188>.
- Moldes, C.A., Medici, L.O., Abrahão, O.S., Tsai, S.M., Azevedo, R.A., 2008. Biochemical responses of glyphosate resistant and susceptible soybean plants exposed to glyphosate. *Acta Physiol. Plant.* 30, 469–479. <https://doi.org/10.1007/s11738-008-0144-8>.
- Orcaray, L., Igal, M., Marino, D., Zabalza, A., Royuela, M., 2010. The possible role of quinate in the mode of action of glyphosate and acetolactate synthase inhibitors. *Pest Manag. Sci.* 66, 262–269. <https://doi.org/10.1002/ps.1868>.
- Pérez-López, U., Pinzino, C., Quartacci, M.F., Ranieri, A., Sgherri, C., 2014. Phenolic composition and related antioxidant properties in differently colored lettuces: a study by electron paramagnetic resonance (EPR) kinetics. *J. Agric. Food Chem.* 62, 12001–12007. <https://doi.org/10.1021/jf503260v>.
- Radwan, D.E.M., Fayed, K.A., 2016. Photosynthesis, antioxidant status and gas-exchange are altered by glyphosate application in peanut leaves. *Photosynthetica* 54, 307–316. <https://doi.org/10.1007/s11099-016-0075-3>.
- Romero-Puertas, M.C., Palma, J.M., Gómez, M., Del Río, L.A., Sandalio, L.M., 2002. Cadmium causes the oxidative modification of proteins in pea plants. *Plant Cell Environ.* 25, 677–686. <https://doi.org/10.1046/j.1365-3040.2002.00850.x>.
- Romero-Puertas, M.C., Rodríguez-Serrano, M., Corpas, F.J., Gómez, M., Del Río, L.A., Sandalio, L.M., 2004. Cadmium-induced subcellular accumulation of O<sub>2</sub> and H<sub>2</sub>O<sub>2</sub> in pea leaves. *Plant Cell Environ.* 27, 1122–1134. <https://doi.org/10.1111/j.1365-3040.2004.01217.x>.
- Romero, D.M., Ríos de Molina, M.C., Juárez, Á.B., 2011. Oxidative stress induced by a commercial glyphosate formulation in a tolerant strain of *Chlorella kessleri*. *Ecotoxicol. Environ. Saf.* 74, 741–747. <https://doi.org/10.1016/j.ecoenv.2010.10.034>.
- Schützendübel, A., Nikolova, P., Rudolf, C., Polle, A., 2002. Cadmium and H<sub>2</sub>O<sub>2</sub>-induced oxidative stress in *Populus × canadensis* roots. *Plant Physiol. Biochem.* 40, 577–584. [https://doi.org/10.1016/S0981-9428\(02\)01411-0](https://doi.org/10.1016/S0981-9428(02)01411-0).
- Sergieiev, I.G., Alexieva, V.S., Ivanov, S.V., Moskova, I.I., Karanov, E.N., 2006. The phenylurea cytokinin 4PU-30 protects maize plants against glyphosate action. *Pestic. Biochem. Physiol.* 85, 139–146. <https://doi.org/10.1016/j.pestbp.2006.01.001>.
- Soares, C., Pereira, R., Spormann, S., Fidalgo, F., 2019. Is soil contamination by a glyphosate commercial formulation truly harmless to non-target plants? – evaluation of oxidative damage and antioxidant responses in tomato. *Environ. Pollut.* 247, 256–265. <https://doi.org/10.1016/j.envpol.2019.01.063>.
- Steffens, B., Steffen-Heins, A., Sauter, M., 2013. Reactive oxygen species mediate growth and death in submerged plants. *Front. Plant Sci.* 4, 1–7. <https://doi.org/10.3389/fpls.2013.00179>.
- Stephenie, S., Chang, Y.P., Gnanasekaran, A., Esa, N.M., Gnanaraj, C., 2020. An insight on superoxide dismutase (SOD) from plants for mammalian health enhancement. *J. Funct. Foods* 68, 103917. <https://doi.org/10.1016/j.jff.2020.103917>.
- Takano, H.K., Beffa, R., Preston, C., Westra, P., Dayan, F.E., 2019. Reactive oxygen species trigger the fast action of glufosinate. *Planta* 249, 1837–1849. <https://doi.org/10.1007/s00425-019-03124-3>.
- Vélez-Gavilán, J., 2019. *Amaranthus palmeri* (Palmer amaranth) [WWW Document]. *Invasive Species Compend.* <https://doi.org/10.1079/ISC.4649.20203482869>.
- Verma, S., Dubey, R.S., 2003. Lead toxicity induces lipid peroxidation and alters the activities of antioxidant enzymes in growing rice plants. *Plant Sci.* 164, 645–655. [https://doi.org/10.1016/S0168-9452\(03\)00022-0](https://doi.org/10.1016/S0168-9452(03)00022-0).
- Vivancos, P.D., Driscoll, S.P., Bulman, C.A., Ying, L., Emami, K., Treumann, A., Mauve, C., Noctor, G., Foyer, C.H., 2011. Perturbations of amino acid metabolism associated with glyphosate-dependent inhibition of shikimic acid metabolism affect cellular redox homeostasis and alter the abundance of proteins involved in photosynthesis and photorespiration. *Plant Physiol.* 157, 256–268. <https://doi.org/10.1104/pp.111.181024>.
- Yan, L.J., Orr, W.C., Sohal, R.S., 1998. Identification of oxidized proteins based on sodium dodecyl sulfate-polyacrylamide gel electrophoresis, immunochemical detection, isoelectric focusing, and microsequencing. *Anal. Biochem.* 263, 67–71. <https://doi.org/10.1006/abio.1998.2799>.
- Yu, H., Peng, J., Cao, X., Wang, Y., Zhang, Z., Xu, Y., Qi, W., 2021. Effects of microplastics and glyphosate on growth rate, morphological plasticity, photosynthesis, and oxidative stress in the aquatic species *Salvinia cucullata*. *Environ. Pollut.* 279, 116900. <https://doi.org/10.1016/j.envpol.2021.116900>.
- Zhong, G., Zhou, J., Liu, Y., Cai, H., Liu, N., Pang, Y., Wu, Z., 2018. Separate and combined effects of glyphosate and copper on growth and antioxidative enzymes in *Salvinia natans* (L.). *Sci. Total Environ.* 655, 1448–1456. <https://doi.org/10.1016/j.scitotenv.2018.11.213>.
- Zinellu, A., Sotgia, S., Posadino, A.M., Pasciu, V., Perino, M.G., Tadolini, B., Deiana, L., Carru, C., 2005. Highly sensitive simultaneous detection of cultured cellular thiols by laser induced fluorescence-capillary electrophoresis. *Electrophoresis* 26, 1063–1070. <https://doi.org/10.1002/elps.200406191>.
- Zulet, A., Gil-Monreal, M., Zabalza, A., van Dongen, J.T., Royuela, M., 2015. Fermentation and alternative oxidase contribute to the action of amino acid biosynthesis-inhibiting herbicides. *J. Plant Physiol.* 175, 102–112. <https://doi.org/10.1016/j.jplph.2014.12.004>.